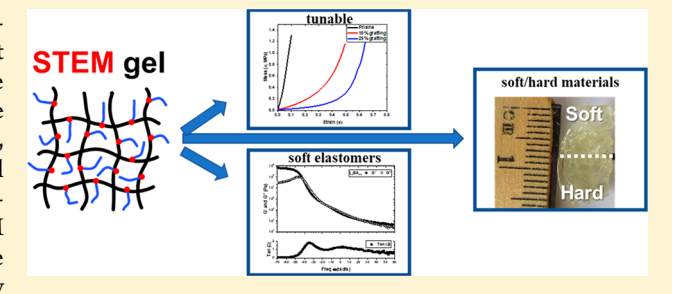
ACTOMORULES © Cite This: Macromolecules 2018, 51, 9184–9191

Structurally Tailored and Engineered Macromolecular (STEM) Gels as Soft Elastomers and Hard/Soft Interfaces

Julia Cuthbert, Tao Zhang, Santidan Biswas, Mateusz Olszewski, Sivaprakash Shanmugam, Travis Fu,[†] Eric Gottlieb,[†] Tomasz Kowalewski,*^{,†} Anna C. Balazs,*^{,‡} and Krzysztof Matyjaszewski*,†®

Supporting Information

ABSTRACT: Structurally tailored and engineered macromolecular (STEM) gels are polymer networks containing latent initiator sites available for postsynthesis modifications. The STEM gels presented here were synthesized by reversible addition-fragmentation chain transfer (RAFT) polymerization, and the network was modified by grafting soft poly(n-butyl acrylate) (PBA) side chains via atom transfer radical polymerization (ATRP) to create supersoft materials. Modified STEM gels with low Young's moduli (E = 590-220 kPa) were produced, and the mechanical properties were tunable by



varying the grafting density and side chain length. Dissipative particle dynamics (DPD) simulations were used to gain insight into side chain mobility in the network. This approach was also used to made soft elastomers (E = 42 kPa), which could withstand 100% shear strain without permanent deformation. Using spatial control, single-piece materials with hard or soft domains were synthesized.

INTRODUCTION

Polymeric elastomers are soft, deformable networks that open up new possibilities for stretchable electronics, energy dissipation, 2,3 soft robotics, 4 and tissue engineering. 5 Fabricating technologically important elastomers can, however, be challenging because certain applications require materials with tunable mechanical properties or a single sample that displays distinct regions with different mechanical behavior. The mechanical properties of elastomers are predominately related to the cross-link density, which is inversely related to the polymer molecular weight between cross-links (M_x) . Varying M_x provides a means of tailoring the material mechanics. Increasing M_r leads to a decrease in the cross-link density and results in a more deformable network. In the dry state, chain entanglements effectively act as cross-links and thus reduce the network deformability.

The mechanical behavior of the network can be also tailored through the addition of small-molecule additives (e.g., solvents), which can act as softening agents. Such additives typically swell polymer chains, increase their mobility and release some entanglements. Gels swollen in water (hydrogels) or oil (organogels) can exhibit very low elastic and shear moduli, comparable to biological tissues.8 Some limitations of this approach include potential embrittlement of the material due to the stretching of polymer chains and/or the loss of the small molecule additive through evaporation.

Swollen gels can be toughened through the incorporation of a secondary macromolecular component, which leads to the formation of double or interpenetrating polymer networks (DN, IPN). The presence of this secondary component can produce a high level of mechanical microheterogeneity and can cause toughening of the material through microyielding. Recently, "biphasic synergistic gels" were prepared by emulsion polymerization to create a novel microinclusion architecture, which resulted in superior strength and extensibility compared to a traditional hydrogel. 10 It should be pointed out that formation of the secondary network is associated with the introduction of more cross-link sites, which typically leads to the increase of network rigidity.

Introduction of the secondary macromolecular component does not, however, have to involve formation of the secondary network. The secondary chains can be simply grown within the primary network without any covalent attachment or can be grafted from the embedded initiator sites. If such a grafted secondary polymer is characterized by high conformational mobility and favorably interacts with the primary network, it can effectively mimic the presence of softening small molecular additives, such as solvents, without the possibility of its

Received: August 31, 2018 Revised: October 24, 2018 Published: November 8, 2018

Department of Chemistry, Center for Macromolecular Engineering, Carnegie Mellon University, 4400 Fifth Avenue, Pittsburgh, Pennsylvania 15213, United States

^{*}Chemical Engineering Department, University of Pittsburgh, Pittsburgh, Pennsylvania 15261, United States

undesirable escape from the network. ^{11,12} The architecture of such a network is reminiscent of polymer brushes, with the network acting as a backbone grafted with polymer side chains. For good control of the resulting polymer material, it is desirable to grow the secondary chains using a method that ensures good control over their lengths, such as atom transfer radical polymerization (ATRP). ^{13,14} In recent years, this technique has been used to synthesize supersoft bottlebrush elastomers with a shear modulus on the order of 10⁴ Pa, ^{15,16} which typically can be accomplished only by swelling the network with a solvent. It has also been used more recently to synthesize complex-architecture soft elastomers, which show elongations at break far exceeding the limits predicted by well-established inverse empirical correlation between the materials' modulus and extensibility. ¹⁷

Another example of polymer networks with secondary dangling chains are structurally tailored and engineered macromolecular (STEM) gels that are highly tunable materials capable of postsynthesis modifications and were developed in recent years by our groups. ^{18,19} STEM gels are polymer networks containing latent initiator sites (inimers). The precursor network is made by reversible addition—fragmentation transfer (RAFT) polymerization containing ATRP inimers, available for subsequent orthogonal modification. ^{20,21} In our previous report on soft elastomers, an extra step was required to introduce the ATRP initiator sites after the primary network synthesis. ¹¹ In this work, primary STEM gels were used as templates for soft elastomers by grafting poly(*n*-butyl acrylate) (PBA) side chains from the inimers. These low glass transition temperature side chains effectively act as solvent/diluent.

Here, we describe how to achieve considerable spatiotemporal control over the STEM gels and thereby expand the field of photodriven additive manufacturing. ^{22–25} In particular, by employing photoinduced ATRP, ^{26–28} we demonstrate how the STEM gel can be transformed from a hard network to a soft elastomer by postsynthesis. We also show how to harness the STEM gels to create elastomers that contain both hard and soft domains and, thus, provide a new means of addressing the need for a single polymeric sample that contains mechanically distinct domains. ^{29–31}

■ EXPERIMENTAL SECTION

Materials. Benzyl methacrylate (BzMA, 96%, Aldrich), n-butyl acrylate (BA, 99%, Aldrich), n-butyl methacrylate (BMA, 99%, Aldrich), and poly(ethylene glycol) dimethacrylate (PEO₇₅₀DMA, average molecular weight 750, Aldrich) were passed through basic alumina column to remove radical inhibitors prior to use. 2,2'-Azobis(isobutyronitrile) (AIBN, Aldrich, 98%) was recrystallized from ethanol. 1-Butanol (Aldrich, 99%), dichloromethane (DCM, ACS grade, Fisher Scientific), copper(II) bromide (CuBr₂, 99%, Aldrich), 2,2'-azobis(4-methoxy-2,4-dimethylvaleronitrile) (V70, Wako), 4-cyano-4[(dodecylsulfanylthiocarbonyl)sulfanyl]pentanoic acid (CDTP, 97%, Aldrich), 4-cyano-4-(phenylcarbonothioylthio)pentanoic acid (CPADB, 97%, Aldrich), ethyl α -bromoisobutyrate (EBiB, 98%, Aldrich), sodium bicarbonate (Fischer Chemicals), fuming sulfuric acid (Alfa Aesar, 20% sulfuric acid, 80% free SO₃⁻), toluene (HPLC grade, Fisher Scientific), N,N-dimethylformamide (DMF, ACS grade, Fisher Scientific), deuterated chloroform (CDCl₃, 99.8%, Cambridge Isotope Laboratories), and tris[2-(dimethylamino)ethyl]amine (Me6TREN, Aldrich) were used as received. HEMA-iBBr was synthesized as previously reported. 19 Glass slides (Borosilicate, McMaster-Carr) were treated with Rain-X antiadhesive to prevent gel adhesion to the glass. Molds were made by sandwiching

a silicone rubber seal (McMaster-Carr extreme temperature silicone rubber 1 mm thick) between two glass plates.

Synthesis. STEM-0 Gels. A linear model and subsequent brush model were prepared and characterized by ¹H NMR and GPC (Figures S1-S3 and Scheme S1). For the STEM-0 with inimer = 10% (I_{10}) , the BMA monomer (3.4356 g, 24.2 mmol, 900 equiv), crosslinker PEO₇₅₀DMA (59.4 mg, 0.08 mmol, 3 equiv), HEMA-iBBr inimer (0.75 g, 2.7 mmol, 100 equiv), and the RAFT agent, CPADB (7.5 mg, 0.027 mmol, 1 equiv), were dissolved in toluene (3 mL) with DMF (0.1 mL) as the ¹H NMR internal standard, in a Schlenk flask and degassed by nitrogen sparging for 25 min. The radical initiator, V-10 (1.4 mg, 0.005 mmol, 0.5 equiv), was added under positive nitrogen pressure. The pregel solution was transferred to a degassed vial via a purged syringe. The reaction was started at 46 °C on a heating mantel for 3 days. Conversion was determined by extraction of the unreacted monomer in \mbox{CDCl}_3 and subsequent $^1\mbox{H}$ NMR. The STEM gels were dialyzed in DCM for 5 cycles over 48 h. The obtained gels were first dried under air and then in an oven at 35 °C for 24 h and were finally placed in a desiccator under vacuum.

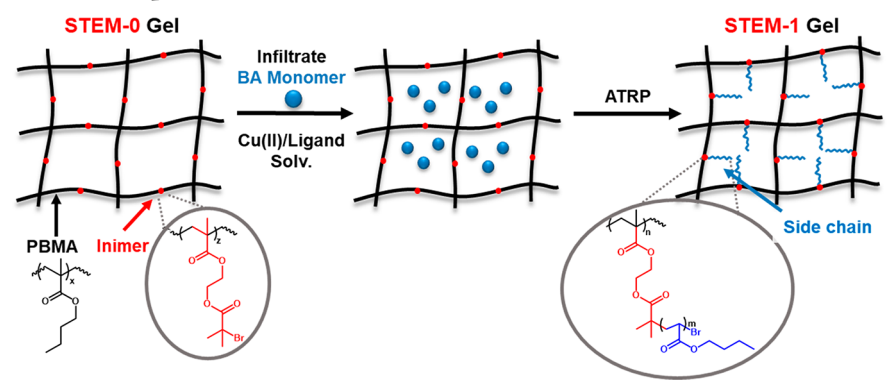
For the STEM-0 with inimer = 25% (I_{25}), the same general procedure was followed with the following conditions: The ratio of reactants was [BMA]/[PEO₇₅₀DMA]/HEMA-iBBr]/[CPADB]/[V-70] = [900]/[4]/[300]/[0.35]; $V_{\rm M}$: $V_{\rm S}$ = 1:1 (Scheme S2). For the hard/soft and hinge materials, an I_{25} STEM gel was prepared with the same molar ratios using CDTP (5.5 mg, 0.016 mmol, 1 equiv) as the RAFT agent and 10 drops of benzyl methacrylate as the Raman spectroscopy internal standard (Scheme S2).

General Procedure for Postsynthesis Modifications by Photo-ATRP. The dried STEM-0 gels were weighted (125-200 mg) and swollen in an infiltration solution containing the BA monomer, catalyst (CuBr₂/Me₆TREN), and solvent (DMF) overnight (18 h) (for details, see Table S1). The infiltrated STEM gels were weighed (swelling ratio = $\frac{W_{\rm S}}{W_{\rm D}}$) and placed in a mold. The mold was covered and degassed under nitrogen for 20 min, and then the infiltrated sample was irradiated with a UV lamp (365 nm, 3.65 mW/ cm²) for 4 h. The STEM-1 gels were dialyzed in DCM for five cycles over 48 h, dried under air and then in an oven at 35 °C for 24 h, and finally placed in a desiccator under vacuum. The gels were weighed again after 5 days in the desiccator. Conversion was estimated by gravimetry. For the hard/soft and hinge materials, the same general procedure was followed. The STEM-0 gels were placed in an infiltration solution containing 100 equiv of BA relative to the calculated moles of inimer present in the STEM-0 sample, and CuBr₂ = 750 ppm; CuBr₂:Me₆TREN = 1:6 in DMF.

Material Characterization. ¹H nuclear magnetic resonance (NMR) measurements were performed on a Bruker Avance 300 MHz spectrometer. Raman microscopy was performed using an NT-MDT Spectra AFM/Raman microscope with a 532 nm laser. The STEM gel spectra were normalized to the integral of intensity between 988 and 1010 cm⁻¹ corresponding to the benzyl methacrylate internal standard peak. Molecular weight (M_n) and molecular weight distribution $(D, M_w/M_p)$ were determined by gel permeation chromatography (GPC). The GPC system used a Waters 515 HPLC pump and a Waters 2414 refractive index detector using PSS columns (Styrogel 102, 103, and 105 Å) with THF as the eluent at a flow rate of 1 mL/min at 35 °C using linear poly(methyl methacrylate) (PMMA) standards. A MelodySusie UV lamp was used for the initial experiment for the postsynthesis modifications. The images and videos were taken using a Canon PowerShot ELPH 360 HS digital camera. The videos were analyzed using VirtualDub video editing software and ImageJ image analysis and processing software.

Mechanical properties of the STEM gels were assessed in the dry state (unless otherwise noted) using an Anton Paar MCR-302 rheometer fitted with a parallel plate tool. Disk-shaped gel samples with a thickness of 1-2 mm and diameter D=5-10 mm were subjected to periodic torsional shearing between two parallel plates under a constant normal load of 1 N in the linear viscoelastic response region. The frequency sweeps were performed at room temperature (22 °C) at a constant applied shear strain of 0.1% (γ) over a

Scheme 1. Procedure for Postsynthesis Modification of the STEM-0 Gels (PBMA-stat-Inimer-stat-PEO₇₅₀DMA) by Infiltrating Monomer and Catalyst and Subsequent ATRP to Graft Side Chains from the Inimers (Red), Producing a STEM-1 Gel



frequency range 0.01–100 rad/s. The temperature sweeps were performed at a constant ramp of 2 °C/min with a constant applied shear strain of 0.1% (γ) and a frequency (ω) of 6.28 rad/s (1 Hz). In compression mode, the samples subjected to a normal load increase linearly in time (loading rate = 0.1 N/s) from 0.25 to 20 N for softer samples or start at 1 N and increase to 30 N for more rigid samples. The load vs distance curves were converted into the stress $\sigma = F/(\pi \times (D/2)2)$ and compression strain $\varepsilon = (d_0 - d)/d_0$, where the initial distance between the plates, d_0 (corresponding to the initial sample thickness), was determined by the extrapolation to zero load. For the soft samples, the Young's modulus for compression, E, was calculated by a best fit of the stress—strain curve to the equation describing rubbery elastic behavior: $\sigma_{\rm eng} = E\left(\frac{1}{\lambda} - \frac{1}{\lambda^2}\right) {\rm e}^{A(\lambda-1/\lambda)}$. For the rigid samples, E was calculated as the slope of the initial linear region of constructed stress—strain curves.

Simulations. Dissipative particle dynamics (DPD)^{32–40} were used to model the formation of STEM-0 (pristine) polymer gels and to investigate the mechanical properties of STEM-1 gels under mechanical deformation. Details about the simulations are given in the "Computational Model" section of the Supporting Information.

■ RESULTS AND DISCUSSION

Synthesis of the STEM Gels. The primary STEM-0 gels were prepared in a one-pot synthesis copolymerizing a (meth)acrylate monomer, di(meth)acrylate cross-linker, and (meth)acrylate ATRP initiator (inimer) by RAFT polymerization. The ATRP initiators (inimers) were directly incorporated into the network to avoid multiple postsynthesis modification steps. The pristine networks are termed "STEM-0" and the modified materials "STEM-1" (Scheme 1). Because the goal was to soften the networks and fill the void space with side chains, STEM-0 were synthesized targeting low cross-link density (high M_x) (backbone molecular weight between crosslinks). The statistical number of monomer units between crosslink junctions (n_x) was 300 (the molar ratio of monomer to cross-linker). The inverse grafting density (n_g , the ratio of inimer monomer relative to BMA monomer) and side chain length (n_{sc}) were varied, and their effects on the bulk material properties were investigated.

The STEM-0 networks were used as templates for soft materials. Two sets of STEM-1 gel were prepared based on the 10% (I_{10}) and 25% (I_{25}) inimer concentrations with two different $n_{\rm sc}$. Without the ATRP inimer, no incorporation of the side chains into the network was possible (Figure S4). Extracted linear model chains grown from an infiltrated ATRP initiator, EBiB, in a pure PBMA gel (without inimer copolymerized) showed reasonable dispersity (D) for an innetwork polymerization (Figure S5). The STEM-0s were

Table 1. Pristine PBMA STEM-0 Gels Prepared with a Target $n_x = 300$ and Two Grafting Densities

STEM-0	grafting density (%)	monomer/cross- linker ^b /inimer/ CTA ^c	monomer conv ^d (%)	compressive modulus, E (MPa)
I_{10}	10	900/3/100/1	82	8.6
I_{25}	25	900/4/300/1	63	6.8

^aPercent inimer. ^bCross-linker = PEO₇₅₀DMA. ^cChain transfer agent. ^dExtraction unreacted monomer in CDCl₃ and ¹H NMR.

infiltrated with a solution containing BA monomer, catalyst, and solvent (Table S1 and Table 2). PBA was chosen for its

Table 2. STEM-1 Gels Grafted with PBA Side Chains by Photo-ATRP Targeting Short and Long DPs

label ^a	conv. infiltrated BA monomer (%)	PBA side chains (wt %)	DP side chain $(n_{sc})^b$ (grav)	DP side chain $(n_{sc})^c$ (GPC)	compressive modulus, E (MPa)
$I_{10}BA_{12}$	35	49	12	27	0.59
$I_{10}BA_{17}$	32	57	17	16	0.55
$I_{25}BA_3$	23	31	3	13	0.40
$I_{25}BA_5$	16	48	5	17	0.22

"Refer to Table 1. I + subscript = percentage inimer monomer, and BA + subscript = side chain DP. ^bCalculated based on gravimetric data and assuming 100% inimer initiation efficiency. ^cThe side chains were cleaved from the network and analyzed by GPC (Supporting Information "Side Chain Cleavage from the STEM-1 Networks" and Figure S5).

low glass transition temperature ($T_{\rm g} = -50~{\rm ^{\circ}C}$). The PBA side chains were grown by photoinducted ATRP using UV light (λ = 365 nm) for 4 h. To create short and long side chains, two solutions with different concentrations of BA were prepared. After thorough dialysis and drying, the conversion of BA was determined by gravimetric analysis. Then, the average DP of the PBA side chains was calculated based on the gravimetric data and assuming 100% inimer initiation efficiency (Supporting Information). In addition, the side chains were cleaved from the networks and analyzed by GPC (Supporting Information "Side Chain Cleavage from the STEM-1 Networks" and Figure S5).

Mechanical Properties. To assess the effect of PBA side chains on mechanical properties, the STEM-0 and corresponding STEM-1 networks were characterized by compression testing in the dry state (Figure 1A). The PBA side chains

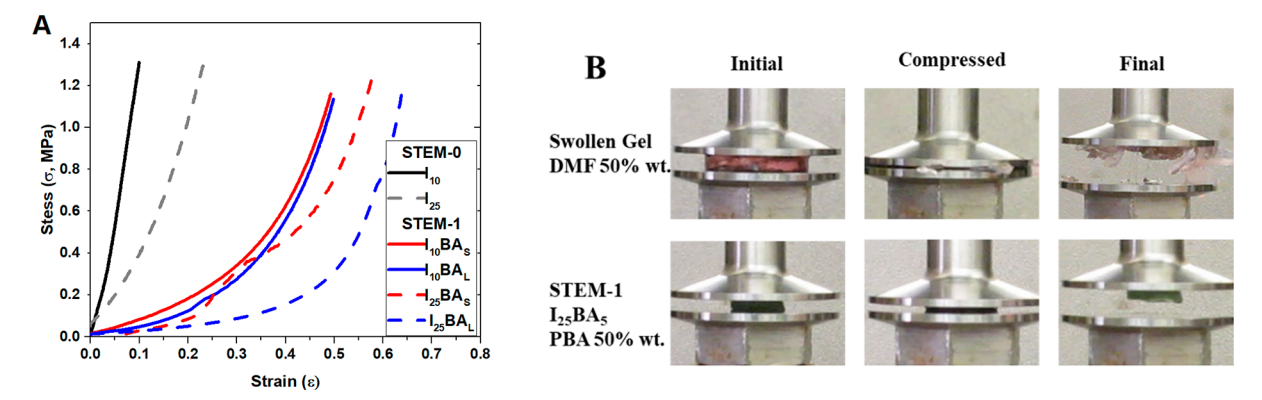


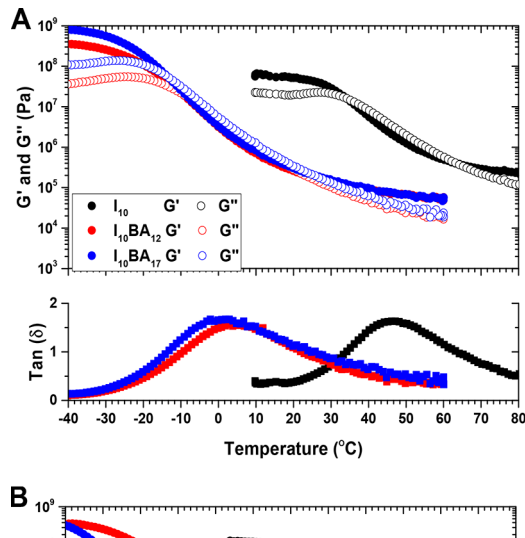
Figure 1. Compressive stress (σ, MPa) -strain (ε) curves of the pristine STEM-0 and modified STEM-1 gels in the dry state from Table 2 (A). Comparison between the compression behavior of a control gel swollen in 50 wt % DMF solvent (B, top) and the dry STEM-1 network $I_{25}BA_5$ containing 48 wt % PBA side chains (B, bottom).

substantially lowered the modulus. In addition, increasing both the inimer concentration and length of the side chains, $n_{\rm sc}$, decreased the compressive modulus, although increasing the $n_{\rm g}$ had a more substantial effect. The STEM-1 $I_{\rm 25}BA_{\rm 3}$, for example, had lower $n_{\rm sc}$ and wt % PBA than either $I_{\rm 10}BA_{\rm 12}$ or $I_{\rm 10}BA_{\rm 17}$, but its modulus (0.40 MPa) was lower than that for the other two samples (see Table 2) Moreover, upon comparison of $I_{\rm 10}BA_{\rm 12}$ and $I_{\rm 25}BA_{\rm 5}$, which had similar wt % PBA, $I_{\rm 25}BA_{\rm 5}$ was softer and more compressible. Depending on the material properties desired, it is possible to tailor and tune the STEM gel properties by controlling the $n_{\rm g}$ and $n_{\rm sc}$.

In the STEM gels, the PBA side chains act as diluent permanently attached to the network (Figures S6 and S7). In effect, despite being solvent-free, the STEM-1 networks will "never dry". Moreover, the PBA side chains soften the networks without embrittlement. To demonstrate this, a control PBMA gel was swollen in 50 wt % DMF and compared to $I_{25}BA_5$ with 48 wt % PBA side chains under a compressive force from 0.25 to 20 N (Figure 1B). The swollen gel failed at a stress of just 0.074 MPa or a normal load of 14.4 N (Figures S7 and S8). In contrast, the STEM-1 networks performed significantly better, enduring higher stress without breaking.

The effect of temperature on the storage (G') and loss (G'')modulus (the elastic and viscous components of the shear modulus, respectively) and the damping factor, $tan(\delta)$ (G"/ G'), was examined (Figure 2A,B). (This is a measure of the energy dissipation of the material.) In agreement with previous reports, the introduction of PBA side chains lowered the STEM-1 network glass transition temperature (T_g) . 11,19 Covalently attaching the side chains to the network resulted in well-defined $tan(\delta)$ peaks, whereas unattached linear chains had a broader plasticizing effect (Figure S9). The STEM-0 gels' T_g was 46 °C, seen in the sharp decrease in G' and G'' and the $tan(\delta)$ maximum value. Lowering the T_g resulted in the STEM-1 networks being soft at room temperature and caused the drop of the G' values in the rubbery plateau region. Moreover, for all STEM-1 samples, the shear moduli increased above the values observed for the pristine networks at lowest temperatures after the vitrification of the secondary chains. This result highlights the importance of side chains' mobility in softening the material.

The temperature sweeps also elucidated the relationship between bulk material properties and side chain length and grafting density. The $\rm I_{10}$ STEM-1 networks with different $n_{\rm sc}$ all



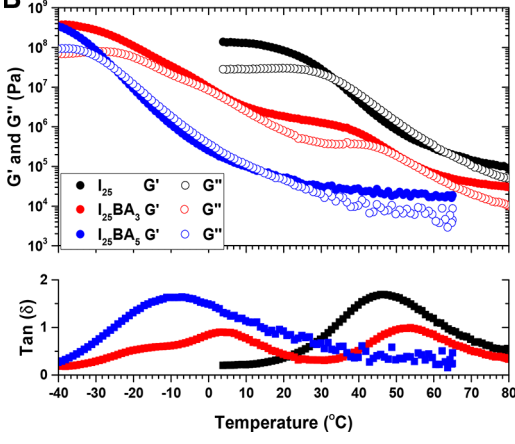


Figure 2. Rheological behavior of the dry STEM-0 (black) and corresponding STEM-1 (red = short n_{sc} ; blue = long n_{sc}) networks. The temperature-dependent behavior of the storage and loss moduli and $\tan(\delta)$ of the I_{10} (A) and I_{25} (B) networks at a constant shear strain $\gamma=0.1\%$ and angular frequency $\omega=6.28$ rad/s.

had glass transition temperatures of ~3 °C (tan(δ) maximum) but different $n_{\rm sc}$. Increasing the number of inimers, however, had a pronounced effect. For instance, the $\rm I_{25}BA_5$ sample had a $T_{\rm g}$ of -10 °C and a lower plateau modulus of 17 kPa, lower than both $\rm I_{10}$ samples. The temperature sweeps also provided an important insight into the $\rm I_{25}BA_3$ behavior observed in the stress—strain curves. Whereas the $\rm I_{10}BA_{12}$, $\rm I_{10}BA_{17}$, and $\rm I_{25}BA_5$ tan(δ) plots showed a single local maximum, the $\rm I_{25}BA_3$ plot

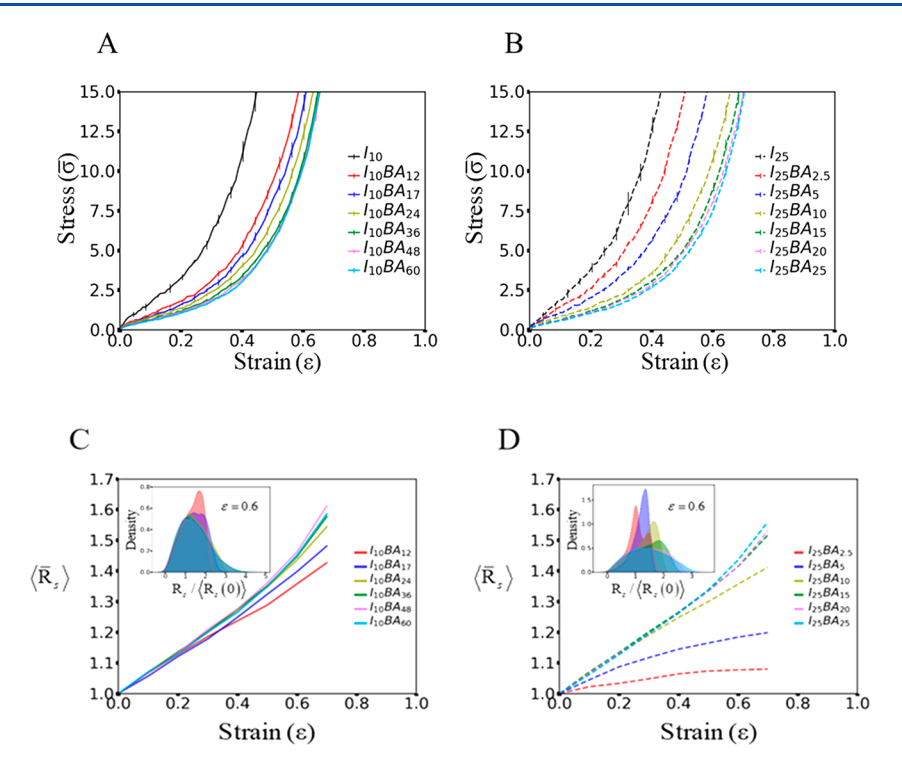


Figure 3. Normalized stress $(\sigma_e/\sigma_{I_{10}BA_1; \iota_{\varepsilon}=0.1})$ vs strain (ε) curves of the STEM-0 and STEM-1 gels, where $\sigma_e = \sigma_t/(1-\varepsilon)$ is the engineering stress (Supporting Information: Computational Model), and $\sigma_{I_{10}BA_{12}; \iota_{\varepsilon}=0.1}$ is the engineering stress of the STEM-1 network $I_{10}BA_{12}$ under strain $\varepsilon=0.1$. (A) Comparison between the compression behaviors of STEM-0 and STEM-1 gels with $n_g=10\%$ and values $n_{sc}=12$, 17, 24, 36, 48, and 60. (B) Comparison between the compression behaviors of STEM-0 and STEM-1 gels with $n_g=25\%$ and $n_{sc}=2.5$, 5, 10, 15, 20, and 25. Normalized averaged two-dimensional end—end distance of side chain $(\langle \overline{R}_s \rangle = \langle R_s(\varepsilon) \rangle/\langle R_s(\varepsilon=0) \rangle)$ vs strain (ε) curves of the modified STEM-1 gels, where $R_s(\varepsilon)$ is the distance between the inimer and the tail bead of single side chain in the yz-plane. (C) Comparison between the $\langle \overline{R}_s \rangle$ of STEM-1 gels with $n_g=10\%$ from (A). (D) Comparison between the $\langle \overline{R}_s \rangle$ of STEM-1 gels with grafting density $n_g=25\%$ from (B). The inset figure plots the density distribution of $R_s(\varepsilon)/\langle R_s(\varepsilon=0)\rangle$ for the given strain $\varepsilon=0.6$. All curves were averaged over five independent runs.

displayed two: 46 and 3 °C. The higher transition suggested the presence of unmodified PBMA domains in which inimer sites did not acquire side chains, possibly being "outcompeted" by other active growth areas under the conditions of low monomer-to-inimer ratio.

Modeling the Effect of Side Chain Length. To study the effect of varying the length of the side chains on the mechanical properties of the STEM gels, the compressive deformation of STEM-0 gels and STEM-1 gels was modeled for different values of $n_{\rm sc}$. The stress for a specific value of strain decreased with an increase in n_{sc} indicating that the side chains soften the networks for both I₁₀ and I₂₅ STEM-1 gels (Figure 3). For example, at strain $\varepsilon = 0.2$, the stress in the $I_{25}BA_5$ STEM-1 gels was a factor of ~2 smaller than that in the I₂₅ STEM-0 gels, and the stress in the I₂₅BA₁₀ gels was roughly 3 times smaller than that in the I_{25} STEM-0 samples. In the STEM-1 gels, the side chains acted as a diluent to fill the void space in the network. Under the applied strain, these side chains effectively extend the pristine gel in the plane perpendicular to the compression and thereby relax the network, in agreement with experimental results (Figure 1A and Figure S10).

From the argument that the side chains act as a diluent, increasing the $n_{\rm sc}$ would be expected to progressively soften and finally collapse the network. In the STEM-1 systems, however, there was a maximum effective length of $n_{\rm sc}$. For the I₁₀STEM-1 gels, the stress—strain curves overlap when $n_{\rm sc} \geq 36$ (Figure 3A), and for the I₂₅ STEM-1 gels, the curves overlap at approximately $n_{\rm sc} = 15$ (Figure 3B). Although the anchored

side chains serve as a diluent, their motion is more restricted than that of a pure solvent for the following reasons: (a) the side chains are attached to the networks at one end, (b) they are restricted by the neighboring side chains, and (c) the spatial heterogeneity of the mesh size and random placement of the initiating sites for the side chain.

Investigating the end-end distance between neighboring side chains (R_s) (Figure 3C,D) further characterized their restricted mobility (for details, see the Supporting Information). The normalized $\langle \overline{R}_s \rangle = \langle R_s(\varepsilon) \rangle / \langle R_s(0) \rangle$ for each side chain length increased as the strain increased (Figure 3C,D); this finding indicated that the side chains were stretched in the plane perpendicular to the compression. The $\langle \overline{R}_s \rangle$ for a specific value of strain increased with an increase in $n_{\rm sc}$ but saturated for higher n_{sc} ($I_{10}BA_{36,48,60}$ and $I_{25}BA_{15,20,25}$). This result indicated that the mobility of the side chains is restricted by steric repulsion from neighboring side chains and physical entanglements with each other. For $I_{10}STEM-1$ gels an increase of $n_{\rm sc} = 17$ to $n_{\rm sc} = 24$ led to a substantial increase of $\langle \overline{R}_s \rangle$ (Figure 3C), whereas for I_{25} STEM-1 gels, the plots for $\langle \overline{R}_{s} \rangle$ of side chain lengths $n_{sc} = 15$ and $n_{sc} = 25$ coincided with each other. At 25% grafting density, the side chains were significantly more constrained and stretched (Figure 3D).

The spatial heterogeneity in molecular weight between cross-links (M_x) in the pristine networks and the random placement of the inimers (see the Supporting Information: "Formation of STEM-0 Gels and STEM-1 Gels") also contributed to the saturation effect in $n_{\rm sc}$ values observed. Polymer networks fabricated via controlled radical polymer-

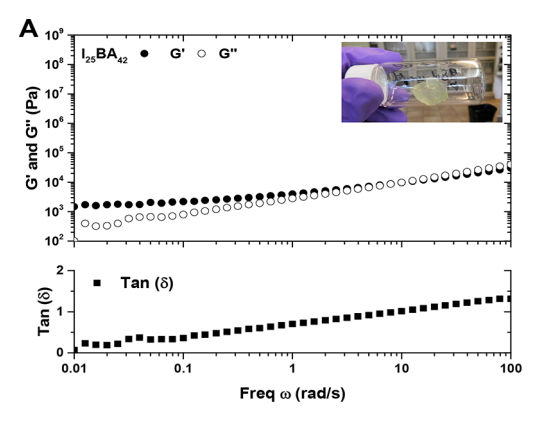
ization exhibit inhomogeneous distribution of cross-links and topological defects, such as dangling chain ends and loops. Rather than using a prefabricated diamond network with uniformly distributed cross-links, the pristine network was simulated using a DPD model that incorporates the ATRP reaction kinetics. Therefore, the polymer network resulting from these simulations displayed a cross-link density distribution. The statement of the polymer network resulting from these simulations displayed a cross-link density distribution.

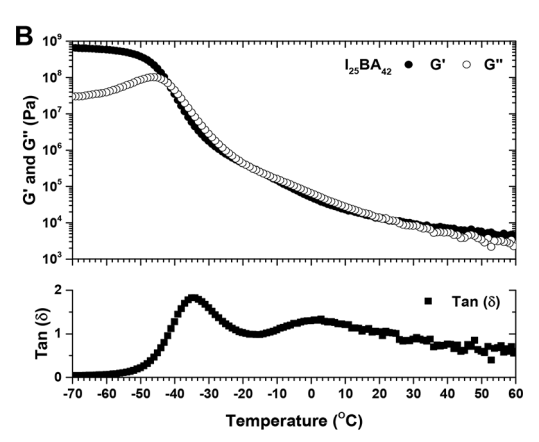
The above information is useful for understanding the results in Figure 3, which shows that the distribution of the side chain end-end distances became broader for higher $n_{\rm sc}$ (insets of Figure 3C,D). This broadened distribution was due to the network spatial heterogeneity; long side chains embedded in sparsely distributed regions (higher M_x) were stretched to a relatively high degree and were primarily responsible for this broadening. Notably, long side chains embedded in regions with relatively high cross-link densities stretched less in constrained space. For lower n_{sc} , the spread of the distribution of the side chain end-end distance was relatively narrow (insets of Figure 3C,D), suggesting that even in the low M_x the short side chains were still stretched to the same degree as in the high M_x regions. Therefore, a saturation effect was observed in which these side chains cannot extend the pristine networks any further to relax the stress.

Supersoft STEM Gel. Given the previous experimental and modeling results, the I₂₅ network with longer side chains was the best temperate for very soft materials. To more closely mimic the supersoft elastomeric properties of previously reported bottlebrushes, 15 a STEM-1 network was prepared consisting of 88 wt % PBA side chains or $n_{\rm sc}$ = 42, $I_{25}BA_{42}$ (Supporting Information). At 25 °C, its equilibrium shear modulus (G' at 0.01 rad/s) was 1.5 kPa (Figure 4A). In the DMA temperature sweeps, the G' led to a rubbery plateau of 4.2 kPa (Figure 4B) comparable to bottlebrush elastomers. The compression testing revealed a soft material with a compressive E = 42 kPa (Figure 4C), comparable to soft biological tissue, like cartilage. 42 This material was comparable to a gel swollen in pure solvent (Figures S7B and 8B) but did not rupture under compression. In addition, his material could withstand shear strains up to 100% before significant deformation was observed (Figure S11).

Interfacing Hard/Soft Materials. The previous samples demonstrated the transformation of the PBMA networks from stiff materials to soft elastomers. Taking advantage of the spatial control afforded by photo-ATRP, two hard/soft interfacial materials were made using a photomask during polymerization (Figure 5A,B). By covering parts of the infiltrated STEM-0 I₂₅ gel, the final STEM-1 had hard and soft sections (Figure 5A, Figures S11 and S12). The STEM network mass increased by 13% after grafting the PBA side chains, and the Raman spectrum showed a 17% increase in the C—H bond intensity (Figure S13). The result was a single-piece material with a difference in modulus of approximately an order of magnitude between the two distinct regions.

In addition, a flexible hinge was produced by modifying the center of the STEM-0 and covering the edges during photo ATRP (Figure 5B). The STEM network mass increased by 7%, and the center, middle transition area, and edges were characterized by DMA. A gradient of Young's modulus from the center to the edge was observed (Figure 5B). A similar trend was observed in the temperature sweeps (Figure S14) in which the $\tan(\delta)$ displays a shift to lower temperatures as the fraction of PBA side chains increased. There was, therefore,





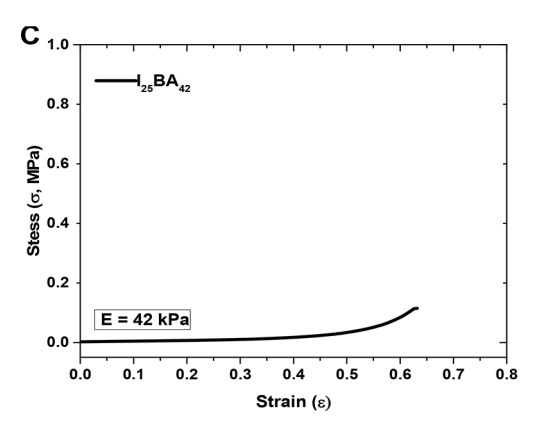


Figure 4. Supersoft STEM-1 $I_{25}BA_{42}$ mechanical properties. Frequency sweep (A) and temperature-dependent behavior. (B). Stress—strain curve (C).

diffusion of radicals into the covered area, and this diffusion resulted in polymerization of PBA side chains. This finding shows the interesting possibility of using STEM gels as template gradient materials.

CONCLUSIONS

The STEM gels were demonstrated to be highly tunable scaffolds for creating soft materials. By adjustment of the grafting density and side chain length, it was possible to control and tailor the final material properties. Moreover, because the PBA side chains could be grown by photomediated polymerization, spatial control over the postsynthesis modification was realized. Hard/soft materials and "hinge" like materials were created without the need for an interfacial linker or gluing agent. Finally, a supersoft STEM-1 network was synthesized

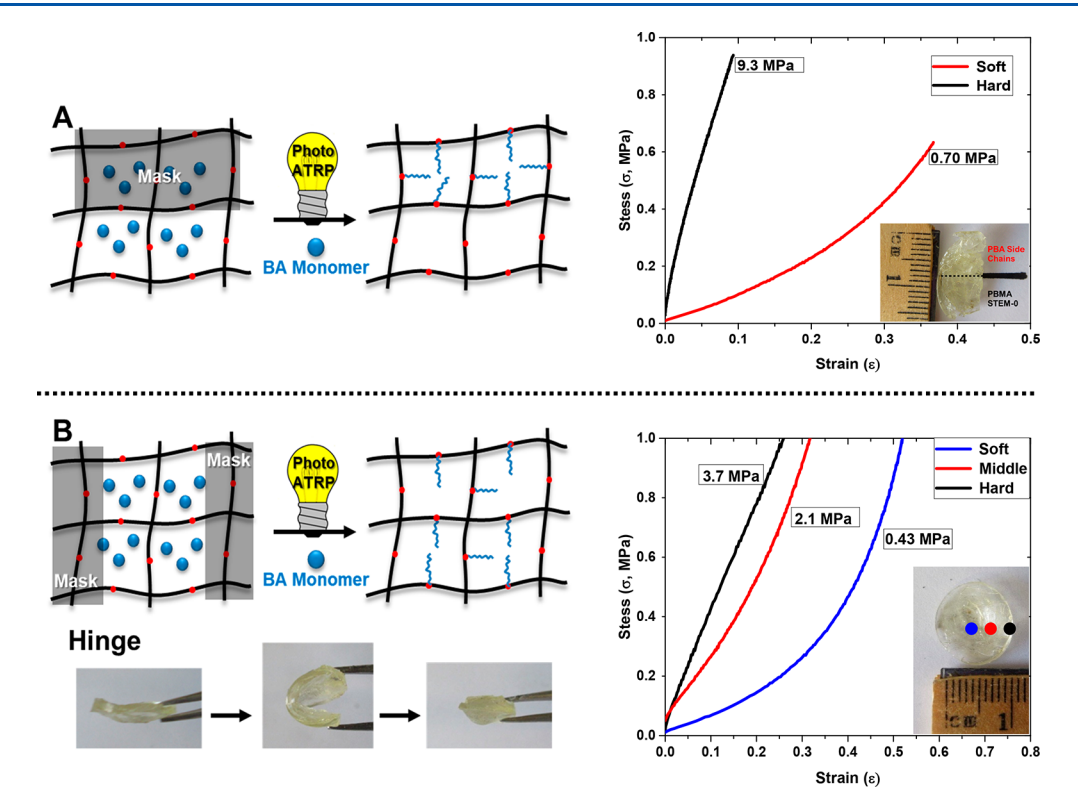


Figure 5. Hard/soft STEM gels with images in the insets. Stress/strain behavior for the half hard, half soft STEM-1 gel (A). Flexible hinge procedure and bending (B). (The yellow color was due to the residual RAFT agent, CDTP.)

with excellent resilience under strain. We envision the STEM gels as templates for soft robotics or wearable electronics, fields in which single-piece materials with a range of mechanical properties and functionalities are required.

ASSOCIATED CONTENT

S Supporting Information

The Supporting Information is available free of charge on the ACS Publications website at DOI: 10.1021/acs.macromol.8b01880.

¹H NMR spectra, STEM gel synthesis details, swelling ratios, GPC traces, DMA frequency and temperature sweeps, stress/strain curves, and computational models (PDF)

AUTHOR INFORMATION

Corresponding Authors

*E-mail: km3b@andrew.cmu.edu.

*E-mail: balazs@pitt.edu.

*E-mail: tomek@andrew.cmu.edu.

ORCID ®

Julia Cuthbert: 0000-0002-0401-8350 Eric Gottlieb: 0000-0002-7948-8031 Tomasz Kowalewski: 0000-0002-3544-554X Anna C. Balazs: 0000-0002-5555-2692

Krzysztof Matyjaszewski: 0000-0003-1960-3402

Notes

The authors declare no competing financial interest.

ACKNOWLEDGMENTS

Financial support from the Department of Energy (Grant ER45998) is gratefully acknowledged. The authors acknowl-

edge use of the Materials Characterization Facility at Carnegie Mellon University supported by grant MCF-677785. The NMR facility at CMU was partially supported by NSF Grants CHE-9808188, CHE-1039870, and CHE-1726525. This research was supported in part by the University of Pittsburgh Center for Research Computing through the resources provided.

REFERENCES

- (1) Wen, H.-F.; Wu, H.-C.; Aimi, J.; Hung, C.-C.; Chiang, Y.-C.; Kuo, C.-C.; Chen, W.-C. Soft Poly(butyl acrylate) Side Chains toward Intrinsically Stretchable Polymeric Semiconductors for Field-Effect Transistor Applications. *Macromolecules* **2017**, *50* (13), 4982–4992.
- (2) Yamazaki, H.; Takeda, M.; Kohno, Y.; Ando, H.; Urayama, K.; Takigawa, T. Dynamic Viscoelasticity of Poly(butyl acrylate) Elastomers Containing Dangling Chains with Controlled Lengths. *Macromolecules* **2011**, *44* (22), 8829–8834.
- (3) Li, Y.; Lian, Q.; Lin, Z.; Cheng, J.; Zhang, J. Epoxy/polysiloxane Intimate Intermixing Networks Driven by Intrinsic Motive Force to Achieve Ultralow-Temperature Damping Properties. *J. Mater. Chem. A* **2017**, *5* (33), 17549–17562.
- (4) Whitesides, G. M. Soft Robotics. *Angew. Chem., Int. Ed.* **2018**, *57* (16), 4258–4273.
- (5) Peppas, N. A.; Hilt, J. Z.; Khademhosseini, A.; Langer, R. Hydrogels in Biology and Medicine: From Molecular Principles to Bionanotechnology. *Adv. Mater.* **2006**, *18* (11), 1345–1360.
- (6) Sarapas, J. M.; Chan, E. P.; Rettner, E. M.; Beers, K. L. Compressing and Swelling To Study the Structure of Extremely Soft Bottlebrush Networks Prepared by ROMP. *Macromolecules* **2018**, *51* (6), 2359–2366.
- (7) Cai, L.-H.; Kodger, T. E.; Guerra, R. E.; Pegoraro, A. F.; Rubinstein, M.; Weitz, D. A. Soft Poly(dimethylsiloxane) Elastomers from Architecture-Driven Entanglement Free Design. *Adv. Mater.* **2015**, *27* (35), 5132–5140.

(8) Rosales, A. M.; Anseth, K. S. The Design of Reversible Hydrogels to Capture Extracellular Matrix Dynamics. *Nat. Rev. Mater.* **2016**, 1, 15012.

- (9) Gong, J. P. Why are double network hydrogels so tough? *Soft Matter* **2010**, *6* (12), 2583–2590.
- (10) Zhao, Z.; Liu, Y.; Zhang, K.; Zhuo, S.; Fang, R.; Zhang, J.; Jiang, L.; Liu, M. Biphasic Synergistic Gel Materials with Switchable Mechanics and Self-Healing Capacity. *Angew. Chem., Int. Ed.* **2017**, *56* (43), 13464–13469.
- (11) Mpoukouvalas, A.; Li, W.; Graf, R.; Koynov, K.; Matyjaszewski, K. Soft Elastomers via Introduction of Poly(butyl acrylate) "Diluent" to Poly(hydroxyethyl acrylate)-Based Gel Networks. *ACS Macro Lett.* **2013**, 2 (1), 23–26.
- (12) Daniel, W. F. M.; Burdyńska, J.; Vatankhah-Varnoosfaderani, M.; Matyjaszewski, K.; Paturej, J.; Rubinstein, M.; Dobrynin, A. V.; Sheiko, S. S. Solvent-free, Supersoft and Superelastic Bottlebrush Melts and Networks. *Nat. Mater.* **2016**, *15*, 183.
- (13) Wang, J. S.; Matyjaszewski, K. Controlled Living Radical Polymerization Atom-Transfer Radical Polymerization in the Presence of Transition-Metal Complexes. *J. Am. Chem. Soc.* **1995**, 117 (20), 5614–5615.
- (14) Matyjaszewski, K.; Xia, J. Atom transfer radical polymerization. *Chem. Rev.* **2001**, *101* (9), 2921–90.
- (15) Neugebauer, D.; Zhang, Y.; Pakula, T.; Sheiko, S. S.; Matyjaszewski, K. Densely-Grafted and Double-Grafted PEO Brushes via ATRP. A Route to Soft Elastomers. *Macromolecules* **2003**, *36* (18), 6746–6755.
- (16) Pakula, T.; Zhang, Y.; Matyjaszewski, K.; Lee, H.-i.; Boerner, H.; Qin, S.; Berry, G. C. Molecular Brushes as Super-soft Elastomers. *Polymer* **2006**, *47* (20), 7198–7206.
- (17) Vatankhah-Varnosfaderani, M.; Daniel, W. F. M.; Everhart, M. H.; Pandya, A. A.; Liang, H.; Matyjaszewski, K.; Dobrynin, A. V.; Sheiko, S. S. Mimicking Biological Stress—Strain Behaviour with Synthetic Elastomers. *Nature* **2017**, *549*, 497.
- (18) Beziau, A.; Fortney, A.; Fu, L. Y.; Nishiura, C.; Wang, H. B.; Cuthbert, J.; Gottlieb, E.; Balazs, A. C.; Kowalewski, T.; Matyjaszewski, K. Photoactivated Structurally Tailored and Engineered Macromolecular (STEM) gels as Precursors for Materials with Spatially Differentiated Mechanical Properties. *Polymer* **2017**, *126*, 224–230.
- (19) Cuthbert, J.; Beziau, A.; Gottlieb, E.; Fu, L.; Yuan, R.; Balazs, A. C.; Kowalewski, T.; Matyjaszewski, K. Transformable Materials: Structurally Tailored and Engineered Macromolecular (STEM) Gels by Controlled Radical Polymerization. *Macromolecules* **2018**, *51* (10), 3808–3817.
- (20) Fenyves, R.; Schmutz, M.; Horner, I. J.; Bright, F. V.; Rzayev, J. Aqueous Self-Assembly of Giant Bottlebrush Block Copolymer Surfactants as Shape-Tunable Building Blocks. *J. Am. Chem. Soc.* **2014**, *136* (21), *7762–7770*.
- (21) Rzayev, J. Synthesis of Polystyrene–Polylactide Bottlebrush Block Copolymers and Their Melt Self-Assembly into Large Domain Nanostructures. *Macromolecules* **2009**, 42 (6), 2135–2141.
- (22) Chen, M.; Gu, Y.; Singh, A.; Zhong, M.; Jordan, A. M.; Biswas, S.; Korley, L. T.; Balazs, A. C.; Johnson, J. A. Living Additive Manufacturing: Transformation of Parent Gels into Diversely Functionalized Daughter Gels Made Possible by Visible Light Photoredox Catalysis. ACS Cent. Sci. 2017, 3 (2), 124–134.
- (23) Mukumoto, K.; Averick, S. E.; Park, S.; Nese, A.; Mpoukouvalas, A.; Zeng, Y.; Koynov, K.; Leduc, P. R.; Matyjaszewski, K. Phototunable Supersoft Elastomers using Coumarin Functionalized Molecular Bottlebrushes for Cell-Surface Interactions Study. *Macromolecules* **2014**, *47* (22), 7852–7857.
- (24) Huq, N. A.; Ekblad, J. R.; Leonard, A. T.; Scalfani, V. F.; Bailey, T. S. Phototunable Thermoplastic Elastomer Hydrogel Networks. *Macromolecules* **2017**, *50* (4), 1331–1341.
- (25) Zhao, F.; Bonasera, A.; Nöchel, U.; Behl, M.; Bléger, D. Reversible Modulation of Elasticity in Fluoroazobenzene-Containing Hydrogels Using Green and Blue Light. *Macromol. Rapid Commun.* **2018**, 39 (1), 1700527.

(26) Konkolewicz, D.; Schroder, K.; Buback, J.; Bernhard, S.; Matyjaszewski, K. Visible Light and Sunlight Photoinduced ATRP with ppm of Cu Catalyst. ACS Macro Lett. 2012, 1 (10), 1219–1223.

- (27) Ribelli, T. G.; Konkolewicz, D.; Pan, X. C.; Matyjaszewski, K. Contribution of Photochemistry to Activator Regeneration in ATRP. *Macromolecules* **2014**, *47* (18), 6316–6321.
- (28) Pan, X. C.; Tasdelen, M. A.; Laun, J.; Junkers, T.; Yagci, Y.; Matyjaszewski, K. Photomediated Controlled Radical Polymerization. *Prog. Polym. Sci.* **2016**, *62*, 73–125.
- (29) Beziau, A.; de Menezes, R.; Biswas, S.; Singh, A.; Cuthbert, J.; Balazs, A.; Kowalewski, T.; Matyjaszewski, K. Combining ATRP and FRP Gels: Soft Gluing of Polymeric Materials for the Fabrication of Stackable Gels. *Polymers* **2017**, *9* (6), 186.
- (30) Beziau, A.; Singh, A.; de Menezes, R. N. L.; Ding, H.; Simakova, A.; Kuksenok, O.; Balazs, A. C.; Kowalewski, T.; Matyjaszewski, K. Miktoarm star copolymers as interfacial connectors for stackable amphiphilic gels. *Polymer* **2016**, *101*, 406–414.
- (31) Argun, A.; Gulyuz, U.; Okay, O. Interfacing Soft and Hard Materials with Triple-Shape-Memory and Self-Healing Functions. *Macromolecules* **2018**, *51* (7), 2437–2446.
- (32) Hoogerbrugge, P. J.; Koelman, J. M. V. A. Simulating Microscopic Hydrodynamic Phenomena with Dissipative Particle Dynamics. *Europhys. Lett.* **1992**, *19* (3), 155–160.
- (33) Espanol, P.; Warren, P. Statistical-Mechanics of Dissipative Particle Dynamics. *Europhys. Lett.* **1995**, 30 (4), 191–196.
- (34) Groot, R. D.; Warren, P. B. Dissipative Particle Dynamics: Bridging the Gap Between Atomistic and Mesoscopic Simulation. *J. Chem. Phys.* **1997**, *107* (11), 4423–4435.
- (35) Fedosov, D. A.; Pivkin, I. V.; Karniadakis, G. E. Velocity Limit in DPD Simulations of Wall-Bounded Flows. *J. Comput. Phys.* **2008**, 227 (4), 2540–2559.
- (36) Yong, X.; Simakova, A.; Averick, S.; Gutierrez, J.; Kuksenok, O.; Balazs, A. C.; Matyjaszewski, K. Stackable, Covalently Fused Gels: Repair and Composite Formation. *Macromolecules* **2015**, *48* (4), 1169–1178.
- (37) Biswas, S.; Singh, A.; Beziau, A.; Kowalewski, T.; Matyjaszewski, K.; Balazs, A. C. Modeling the Formation of Layered, Amphiphilic Gels. *Polymer* **2017**, *111*, 214–221.
- (38) Yong, X.; Kuksenok, O.; Matyjaszewski, K.; Balazs, A. C. Harnessing Interfacially-Active Nanorods to Regenerate Severed Polymer Gels. *Nano Lett.* **2013**, *13* (12), 6269–6274.
- (39) Singh, A.; Kuksenok, O.; Johnson, J. A.; Balazs, A. C. Tailoring the Structure of Polymer Networks with Iniferter-Mediated Photogrowth. *Polym. Chem.* **2016**, *7* (17), 2955–2964.
- (40) Sirk, T. W.; Slizoberg, Y. R.; Brennan, J. K.; Lisal, M.; Andzelm, J. W. An Enhanced Entangled Polymer Model for Dissipative Particle Dynamics. *J. Chem. Phys.* **2012**, *136* (13), 134903.
- (41) Di Lorenzo, F.; Seiffert, S. Nanostructural heterogeneity in polymer networks and gels. *Polym. Chem.* **2015**, *6* (31), 5515–5528.
- (42) Levental, I.; Georges, P. C.; Janmey, P. A. Soft biological materials and their impact on cell function. *Soft Matter* **2007**, 3 (3), 299–306.